CHEMISTRY

Binding energy of solvated electrons and retrieval of true UV photoelectron spectra of liquids

Junichi Nishitani, Yo-ichi Yamamoto*, Christopher W. West, Shutaro Karashima, Toshinori Suzuki†

The electronic energy and dynamics of solvated electrons, the simplest yet elusive chemical species, is of interest in chemistry, physics, and biology. Here, we present the electron binding energy distributions of solvated electrons in liquid water, methanol, and ethanol accurately measured using extreme ultraviolet (EUV) photoelectron spectroscopy of liquids with a single-order high harmonic. The distributions are Gaussian in all cases. Using the EUV and UV photoelectron spectra of solvated electrons, we succeeded in retrieving sharp electron kinetic energy distributions from the spectra broadened and energy shifted by inelastic scattering in liquids, overcoming an obstacle in ultrafast UV photoelectron spectroscopy of liquids. The method is demonstrated for the benchmark systems of charge transfer to solvent reaction and ultrafast internal conversion of hydrated electron from the first excited state.

INTRODUCTION

A hydrated electron (e^-_{aq}), a trapped electron in liquid water, is the simplest reducing reagent in aqueous chemistry. This intriguing species was identified by Hart and Boag in 1962 by pulse radiolysis of liquid water (*1*). As e^-_{aq} is generated in a living cell by radiation impact, it has been extensively studied in radiation chemistry. e^-_{aq} is also observed as a product of electron transfer reactions from photoexcited molecules in aqueous solutions. Nonetheless, the structure (*2*) and dynamics (*3*) of e^-_{aq} are still poorly understood.

The electron binding energy (eBE) is the key quantity that determines reducing power of e^-_{aq}. In 1990, Coe *et al.* (*4*) studied vertical electron binding energies (VBEs; the peak energy of eBE distribution) of water cluster anions generated in molecular beams and predicted the VBE of e^-_{aq} in bulk water to be 3.3 eV. However, it is still debated whether an excess electron is internally bound or trapped on the surface of these clusters (*5*–*7*). If the latter, the VBE predicted using clusters must be incorrect. Thus, it was necessary to directly measure VBE of e^-_{aq} in bulk water.

In 2010, four research groups independently reported the VBE of e^-_{aq} using photoelectron spectroscopy of liquid microjets (*8*–*11*). All research groups reported VBEs of 3.3 to 3.7 eV, which were in fair agreement with the prediction by Coe *et al.* (*4*). However, this did not solve the problem entirely. Yamamoto *et al.* (*12*) showed that these experimental estimates of VBE are possibly inaccurate because the electron kinetic energy (eKE) is altered by inelastic scattering in liquid before emission from the liquid-gas interface. To obtain the correct eBE value, Luckhaus *et al.* (*13*) performed Monte Carlo simulations of electron scattering in liquid water and indicated that the VBE is best estimated to be 3.7 eV. The calculated eBE distribution exhibited a shoulder on the high eBE side.

The present study is aimed at accurate experimental measurement of the eBE distribution of e^-_{aq} to examine the validity of theoretical analysis by Luckhaus *et al.* (*13*) and also at similar measurements for solvated electron (e^-_{solv}) in methanol and ethanol, for which Monte Carlo simulation has not been performed owing to the lack of information on scattering cross sections. To this end, we used ultrafast photoelectron spectroscopy with extreme ultraviolet (EUV) probe pulses. In the EUV and soft x-ray region, the cross sections of elastic and electron-vibron inelastic scattering decline, while electron-electron inelastic scattering increases (*14*). Consequently, the primary (intact) and the secondary (scattered) eKE distributions are separated, and eBE distribution is accurately obtained from the former (*15*–*17*). After we present the correct eBE distributions for e^-_{solv}, we demonstrate the utilization of these distributions for retrieval of sharp spectral features from UV photoelectron spectra of solutions spectrally blurred by inelastic scattering effects. The retrieval method substantially improves the performance of the ultrafast UV photoelectron spectroscopy of liquids.

Our experiment is illustrated in Fig. 1A. We introduced a continuous liquid microjet of NaI solutions in water, methanol, or ethanol into a photoionization chamber through a fused silica capillary with a 15- to 25-μm inner diameter and excited the liquid microjet using 240- or 227-nm pulses to create e^-_{solv}. Their photoelectron spectra were measured using 44.4-nm (27.9 eV) pulses and a 1.3-m-long magnetic bottle time-of-flight (TOF) photoelectron spectrometer.

RESULTS AND DISCUSSION

EUV photoelectron spectroscopy of e^-_{solv}

Figure 1B shows the photoelectron spectrum of an aqueous 0.5 M NaI solution measured using the 240-nm pump and 44.4-nm probe pulses. The pump-probe delay time was 5 ps, and the spectrum was integrated for 1.8×10^8 shots. The pump pulse promoted I^- to a charge–transfer–to–solvent (CTTS) state, from which an electron is released and thermalized in less than 5 ps (*18*–*20*). After 5 ps, e^-_{aq} has only weak interactions with a neutral I atom, and eBE exhibits no further change. The least squares fitting of the spectrum provides an almost perfect Gaussian centered at 3.76 ± 0.05 eV with a full width at half maximum (FWHM) of 1.02 ± 0.04 eV (Fig. 1C). The same Gaussian distribution centered at 3.77 ± 0.10 eV with an FWHM of 1.02 ± 0.07 eV was also observed using different probe photon energy of 29.45 eV (42.1 nm). The shoulder theoretically indicated by Luckhaus *et al.* (*13*) was not identified. Thus, the Monte Carlo simulations were sufficiently accurate to retrieve VBE but not as for the shape of the eBE distribution.

Similarly, Fig. 1 (D and E) respectively shows the photoelectron spectra of e^-_{solv} in methanol and ethanol. The former was measured

Department of Chemistry, Graduate School of Science, Kyoto University, Kitashirakawa-Oiwakecho, Sakyo-Ku, Kyoto, 606-8502, Japan.
*This author contributed equally to this work.
†Corresponding author. Email: suzuki@kuchem.kyoto-u.ac.jp

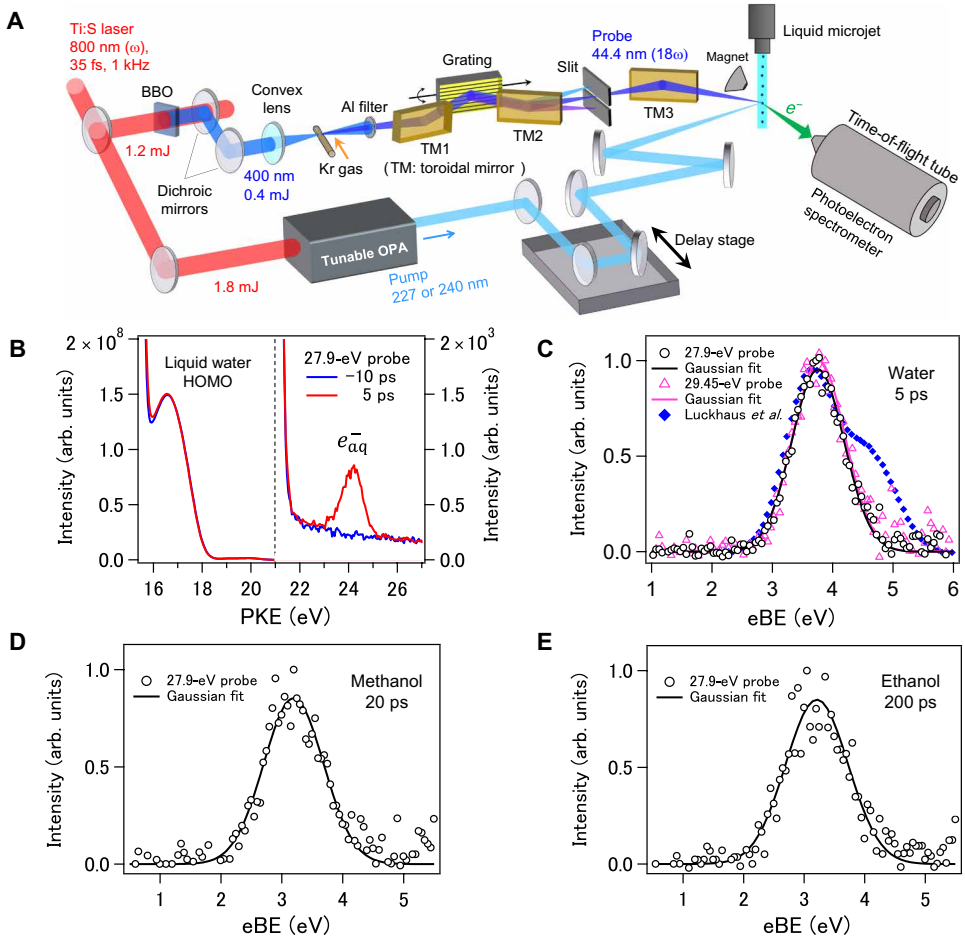

Fig. 1. Experimental apparatus and photoelectron spectra of e^-_{solv}. (**A**) Schematic diagram for UV pump–EUV probe photoelectron spectroscopy. OPA, optical parametric amplifier. BBO, β-BaB_2O_4. (**B**) Photoelectron spectra of an aqueous 0.5 M NaI solution at −10 and 5 ps. The eBE distributions of e^-_{solv} in (**C**) water at 5 ps, (**D**) methanol at 20 ps, and (**E**) ethanol at 200 ps measured in 0.5 M NaI solutions. HOMO, highest occupied molecular orbital.

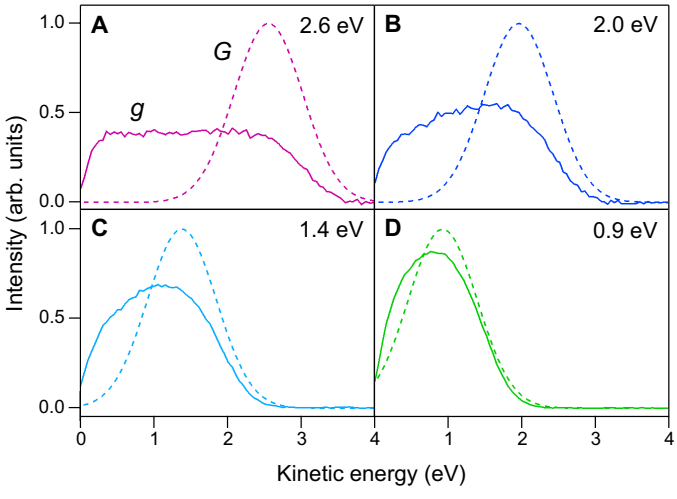

Fig. 2. Electron kinetic energy distribution $G_{\hbar\omega}(E)$ created in conduction band of ethanol by photoexcitation of e^-_{solv} and photoelectron distribution $g_{\hbar\omega}(E)$ measured experimentally. Dashed lines are, respectively, $G_{\hbar\omega}(E)$ for $\hbar\omega$ of (**A**) 5.8, (**B**) 5.2, (**C**) 4.6, and (**D**) 4.1 eV calculated using the eBE distribution of e^-_{solv} in ethanol determined in the present study. The mean kinetic energies of $G_{\hbar\omega}(E)$ are indicated. Solid lines express $g_{\hbar\omega}(E)$ that are the experimental data adopted from (*12*).

with the delay time of 20 ps and integration of more than 7.2×10^7 shots, while the latter with 200 ps and 5.8×10^7 shots. The eBE distributions are well approximated by Gaussian with the center at 3.19 ± 0.04 eV and an FWHM of 1.16 ± 0.13 eV (Fig. 1D) and 3.21 ± 0.06 eV with an FWHM of 1.22 ± 0.10 eV (Fig. 1E). Thermalization of e^-_{solv} in methanol takes longer than 20 ps, in which eBE increases by 0.14 eV as discussed later. We measured eBE distribution for methanol at 100 ps, which has a limited signal-to-noise ratio but further supports this conclusion (see the Supplementary Materials). Thus, VBEs of e^-_{solv} in methanol and ethanol are best estimated to be 3.35 and 3.21 eV, respectively.

As demonstrated here, EUV photoelectron spectroscopy enables accurate measurements of eBE distributions with minimal influence from inelastic scattering effects, while its wide application to solution chemistry may be limited by an extremely low signal level and experimental complexity. Ultrafast UV photoelectron spectroscopy of liquids is much more easily implemented, while its photoelectron spectra are influenced by inelastic scattering in the liquid. If one can correct the inelastic scattering effects, then ultrafast UV photoelectron spectroscopy of liquids will provide more detailed insights into solution chemistry.

Retrieval of eKE distribution before inelastic scattering

To overcome this obstacle in ultrafast UV photoelectron spectroscopy of liquids, we consider using the eBE distributions of e^-_{solv} measured

in this study. The eBE distributions enable us to predict the initial eKE distributions, $G_{\hbar\omega}(E)$, created in the conduction band before inelastic scattering, for various UV photon energies ($\hbar\omega$), through the use of the relation eKE = $\hbar\omega$ − eBE. Here, we define E as the energy measured from the vacuum level; the actual eKE in the conduction band is given by the sum of E and the electron affinity of liquids (the energy difference between the vacuum level and the conduction band minimum). With this definition, E is equal to photoelectron kinetic energy (PKE) after photoemission, and we can focus on the transformation of the distribution function before and after electron scattering. For these photon energies, PKE distributions after inelastic scattering, $g_{\hbar\omega}(E)$, have already been measured (*12*). Examples are shown in Fig. 2. These $G_{\hbar\omega}(E) - g_{\hbar\omega}(E)$ pairs provide us $G_{\hbar\omega}(E) \rightarrow g_{\hbar\omega}(E)$ linear transformation under the influence of inelastic scattering. Then, its inverse transformation enables us to approximately retrieve an eKE distribution before inelastic scattering from a given PKE distribution. In the actual analysis, we expand an experimental PKE time-energy map, $I_{\mathrm{PKE}}(E, t)$, with a set of linearly independent $g_i(E)$ and time-dependent coefficient, $c_i(t)$: $I_{\mathrm{PKE}}(E,t) = \sum_i c_i(t)\, g_i(E)$, where i indicates discrete photon energies. Then, replacing $g_i(E)$ with a corresponding Gaussian-shaped eKE distribution, $G_i(E)$, we retrieve an eKE time-energy map, $I_{\mathrm{eKE}}(E, t)$, as $I_{\mathrm{eKE}}(E,t) = \sum_i c_i(t)\, G_i(E)$.

Ultrafast UV photoelectron spectrum of CTTS reaction

Figure 3 presents PKE maps measured for CTTS reactions from I^- to ethanol, methanol, and water previously reported by Okuyama *et al.* (*18*) along with the retrieved eKE maps and time evolution of VBE value (see the Supplementary Materials for details). The original PKE maps measured for ethanol and methanol are spectrally rather

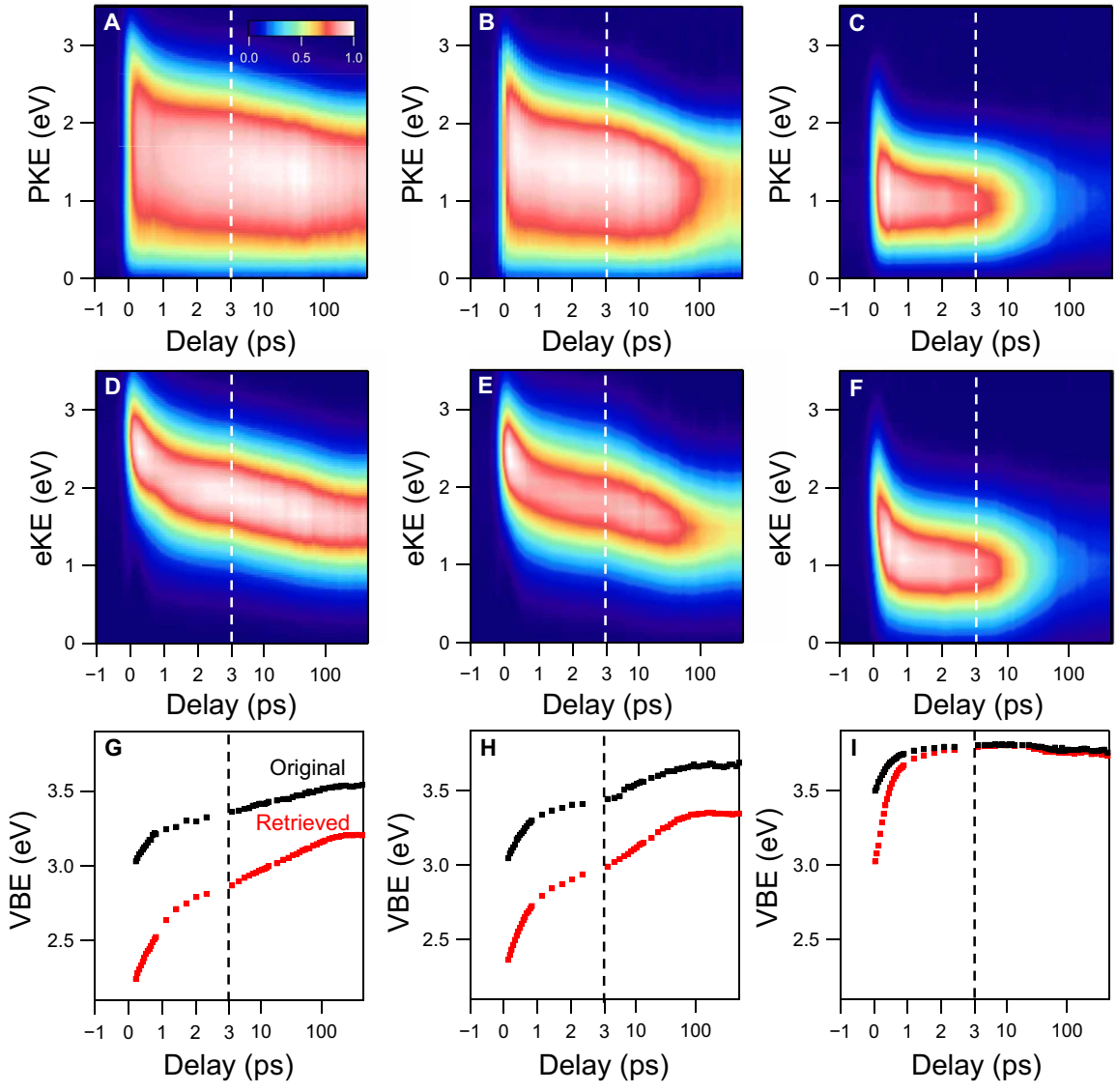

Fig. 3. Ultrafast UV photoelectron spectra of CTTS reaction from I^- to polar protic solvents. PKE time-energy map measured for (**A**) ethanol, (**B**) methanol, and (**C**) water using 226-nm pump and 260-nm probe pulses. (**D** to **F**) The eKE time-energy map retrieved from (A) to (C), respectively. (**G** to **I**) Time evolution of VBE obtained from (A) to (C) (black) and (D) to (F) (red), respectively. The time axes are in linear scale from −1 to 3 ps and in log scale from 3 to 500 ps. Broken lines indicate the boundary of the two scales.

broad. On the other hand, the retrieved spectrum exhibits a narrower spectral width and an upshifted kinetic energy distribution in all cases, as inelastic scattering effects were corrected. Figure 3 (G to I) respectively shows the time evolution of VBE obtained from the original and retrieved spectra of CTTS reaction from I^- to ethanol, methanol, and water. The amount of time-dependent energy shift appears significantly larger for retrieved data than that for original ones, reflecting an inelastic scattering effect. The difference diminishes in the order of ethanol, methanol, and water because VBE increases in this order and eKE diminishes for a given probe photon energy; the inelastic scattering effect diminishes for smaller eKE in this energy region. The ultrafast spectral shift in the CTTS reaction is due to solvation dynamics in the ground state of e^-_{solv}, which is expressed using the following time-correlation function

$$C(t) = \frac{\mathrm{VBE}(t) - \mathrm{VBE}(\infty)}{\mathrm{VBE}(0) - \mathrm{VBE}(\infty)} \quad (1)$$

Figure 3 (G to I) provides $C(t)$ as shown in Fig. 4[(A) ethanol, (B) methanol, and (C) water], respectively. All correlation functions exhibit biexponential decay. The shorter time constants are subpicoseconds to picoseconds, and the longer ones are several tens of picoseconds in alcohols, while subpicosecond and picosecond time constants are found in water. The time constants for original and retrieved data are similar. Comparison of the three solvents illustrates the ultrafast solvation of e^-_{aq}; solvation dynamics of electrons in methanol and ethanol take a considerably longer time than in water, although all these CTTS dynamics occur in the presence of solvation shell for I^-. Thus, the extraction of the correlation functions with solvation time constants provides us deeper insights into the solvation dynamics of an excess electron, while recombination between an excess electron and an iodine atom has already been discussed with a global fit analysis of the spectra or a diffusion equation (*18*–*20*).

Ultrafast UV photoelectron spectrum of internal conversion of e^-_{aq}

Internal conversion from the excited state of e^-_{aq} has been investigated extensively by a number of experimentalists and theorists; however, its dynamics are still in intense debate (*3*, *21*–*26*). The lifetime in the excited state of e^-_{aq} has been estimated with UV photoelectron spectroscopy in some reports (*3*, *27*), while the solvation dynamics in the ground state after the internal conversion has not been examined in detail. In the present study, we performed ultrafast photoelectron spectroscopy of e^-_{aq} with the 720-nm pump pulses and 270-nm probe pulses and applied the retrieval method described above. The e^-_{aq} were created by CTTS from Br^- using 200-nm pulses and thermalized for 500 ps, which was more than sufficient as we have already seen in Fig. 3I. Figure 5A is the eBE time-energy map directly converted from experimental PKE distributions, while Fig. 5B is a similar map using the retrieval method (see the Supplementary Materials for details). The red color corresponds to the pump-probe enhance signal, while the blue color is of the ground-state bleach (depopulation). Both appear with the cross-correlation time of the laser pulses. The enhanced signal appearing in the eBE region of 2 to 3 eV is of the excited electronic state, and it decays very rapidly within ca. 60 fs, while the bleach recovery occurs with a considerably longer time constant. This is because internal conversion creates a nonequilibrium state in the ground state, which undergoes solvation dynamics to reach the thermal equilibrium. For detailed analysis of the experimental data, we have calculated the ground-state bleach signal (Fig. 5C) using the photoelectron spectrum separately measured and retrieved for e^-_{aq} at thermal equilibrium and subtracted it from the retrieved pump-probe photoelectron spectra (Fig. 5B) to obtain the genuine pump-probe enhance signal with the positive sign (Fig. 5D). The time-energy map thus consists of photoemission from the excited and ground electronic states at nonequilibrium, both of which exhibit ultrafast spectral shift owing to solvation dynamics. We separated the map into the contributions from the ground (Fig. 5E) and excited (Fig. 5F) states using their difference in eBE. The latter exhibits ultrafast decay in 64 fs, supporting previous experimental reports (*3*, *27*) and the nonadiabatic model of the dynamics; theoretical calculations predicting the internal conversion lifetime to be on the order of 300 fs likely involve some inaccurate assumptions or approximations (*21*). One can see that the apparent photoemission intensity increases with internal conversion in Fig. 5D; however, note that the photoemission intensity from the excited state is underestimated owing to its lifetime, which is shorter than the cross-correlation time of the laser pulses. We have deconvoluted the cross-correlation time from the measured time-energy map, as shown in Fig. 5G, which reveals a greater photoemission cross section for the excited state than the ground state. Thus, we conclude that the photoemission cross section diminishes upon internal conversion. We are preparing an ultrafast laser system with a higher time resolution to experimentally confirm this conclusion and further elucidate the detail of this fundamental system. From Fig. 5E, $C(t)$ in the ground state is extracted as shown in Fig. 6. The correlation function exhibited biexponential decay with the time constants of 230 and 910 fs. These time constants are in reasonable agreement with the solvation time constants reported for liquid water (*28*–*31*). Liquid water should have an ultrafast inertial response within about 10 fs; however, it cannot be observed in the present case, as the ground state is created with a finite nonadiabatic reaction time from the excited state.

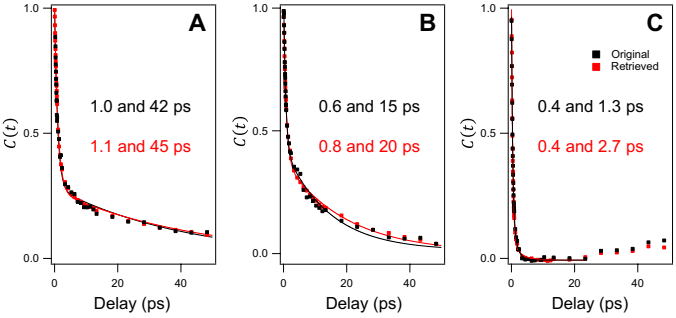

Fig. 4. Time-correlation function C(t) determined from ultrafast UV photoelectron spectra of CTTS reaction from I^- to polar protic solvents. (**A**) ethanol, (**B**) methanol, and (**C**) water. The original (black) and retrieved (red) data points are shown. Time constants and simulated curves in solid line were obtained by the least squares fitting. In (C), an unexpected increase of $C(t)$ by less than 0.1 is seen after 25 ps, which was excluded from the least squares fitting.

CONCLUSION

We have measured accurate eBE distributions of e^-_{solv} in three polar protic solvents by EUV photoelectron spectroscopy and found them to be Gaussian. These distributions were used to retrieve true eBE distributions from UV photoelectron spectra. Our results demonstrate that the retrieval method greatly assists extraction of clear dynamical features from ultrafast UV photoelectron spectra, which were previously blurred and energy shifted by inelastic scattering effects.

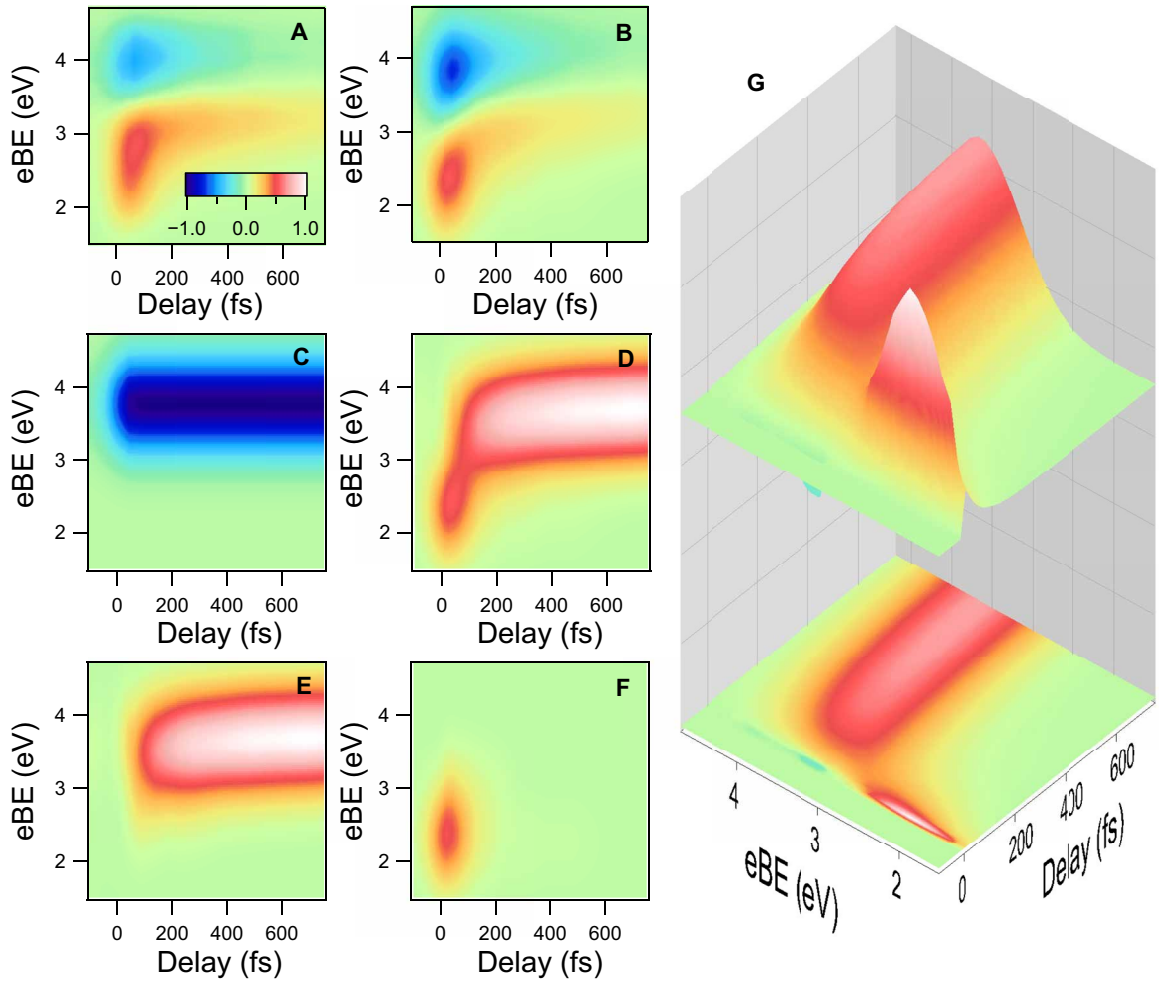

Fig. 5. Ultrafast UV photoelectron spectra of internal conversion of e^-_{aq}. (**A**) eBE time-energy map measured for ultrafast internal conversion of e^-_{aq} with the 720-nm pump and 270-nm probe pulses. (**B**) Retrieved eBE time-energy map. (**C**) Negative signals component calculated from the photoelectron spectrum separately measured and retrieved for e^-_{aq} at thermal equilibrium. (**D**) Positive signal component of the distribution calculated from (B) and (C). (**E**) Signal from the ground state in (D). (**F**) Signal from the excited state in (D). (**G**) Prediction of photoelectron spectra obtained with 5-fs time resolution.

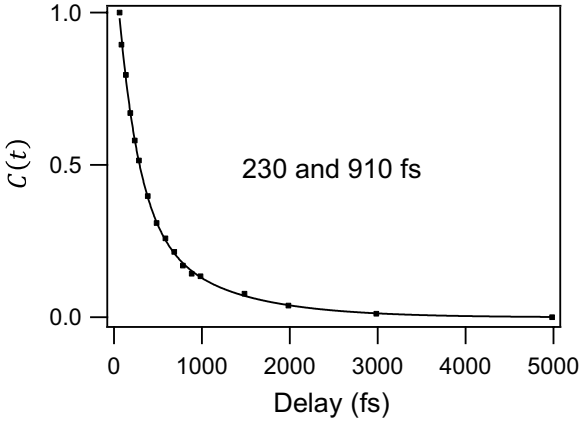

Fig. 6. Time-correlation function *C*(*t*) in the ground state of e^-_{aq} calculated from the data shown in Fig. 5E. Time constants and simulated curves in solid line were obtained by the least squares fitting.

MATERIALS AND METHODS

Ultrafast EUV photoelectron spectroscopy

The schematic diagram of our experimental setup is illustrated in fig. S1A. We introduced a continuous liquid microjet into a photoionization chamber through a 25-μm- and 15-μm-inner-diameter capillary for water and alcohols, respectively. Flow rates were 0.5, 0.25, and 0.15 ml/min for water, methanol, and ethanol, respectively. A Ti:sapphire regenerative amplifier [800 nm (ω), 1 kHz, 35 fs] was used to generate UV pump and EUV probe pulses (*32*). The UV pulses were generated using an optical parametric amplifier and focused on a liquid microjet using an Al concave mirror ($r = 2000$ mm). Pump wavelengths were 240 and 227 nm for water and alcohols, respectively. The maximum UV pulse energies at the sample were 250, 200, and 130 nJ for water, methanol, and ethanol, respectively. The EUV pulses were generated in a Kr gas using 2ω (400 nm, <400 μJ) as a driving laser, and the single-order 18ω (44.4 nm, 27.9 eV) radiation was selected using a home-made time-preserving monochromator based on the design by Frassetto *et al.* (*33*). The EUV pulses

were focused on the sample with a toroidal mirror. The photon flux of 18ω was $<1 \times 10^9$ photons/s; the radiation of the neighboring orders, 14ω and 22ω, was undetected. The experiment was also performed with 19ω (42.1 nm, 29.45 eV) radiation produced by an 800-nm driving laser for comparison. The PKE distribution was measured using a 1.3-m-long magnetic bottle TOF photoelectron spectrometer. A magnetic bottle collected more than 50% of the electrons emitted from the liquid microjet. The energy resolution of the spectrometer was 50 meV. We accelerated photoelectrons from liquid by applying −15 V to the liquid-discharging nozzle and applied a retardation voltage of −27 V to the TOF analyzer to reject electrons with PKE less than 12 eV, which enabled us to remove the gaseous photoelectron bands from the spectral region of interest. The measured PKE was energy-calibrated using a photoelectron band of the highest occupied molecular orbital of each solvent; we used 11.3 (*34*), 9.96, and 9.54 eV measured in our laboratory for water, methanol, and ethanol, respectively.

Ultrafast UV photoelectron spectroscopy

The experimental data on CTTS reaction from I^- to polar protic solvents were published by Okuyama *et al.* (*18*). The internal conversion of e^-_{aq} was newly measured in the present work. A 15-μm-diameter liquid microjet was injected into the vacuum and illuminated at 1 mm downstream from the nozzle with three laser pulses for synthesis, pump, and probe of e^-_{aq}. The driving laser was a 10-kHz one box Ti:sapphire laser with 35-fs pulse duration. The synthesis pulses (200 nm) excited Br^- in a 0.3 M NaBr aqueous solution to create e^-_{aq} by the CTTS reaction. The e^-_{aq} thus created were thermalized for 500 ps, and the pump pulses (720 nm) excited them to the *p* state. Last, the probe pulses (270 nm) interrogated the time evolution of the nonstationary state using photoemission. Since the VBE of liquid water [11.3 eV; (*34*)] is far greater than the probe photon energy, no background signal was created from water. The photoelectrons were detected using a TOF electron energy analyzer with the detection axis perpendicular to the liquid jet and laser beams. All of the laser pulses were linearly polarized, and their polarization directions were parallel to the electron detection axis. The pulse duration of the 200-nm synthesis pulse was stretched using a 45-mm-thick synthetic quartz block to minimize multiphoton excitation. The laser pulse energies were 13, 185, and 41 nJ for the synthesis, pump, and probe pulses, respectively. Streaming potential was canceled by applying a voltage to the liquid-discharging nozzle.

SUPPLEMENTARY MATERIALS

Supplementary material for this article is available at http://advances.sciencemag.org/cgi/content/full/5/8/eaaw6896/DC1

REFERENCES AND NOTES

1. E. J. Hart, J. W. Boag, Absorption spectrum of the hydrated electron in water and in aqueous solutions. *J. Am. Chem. Soc.* **84**, 4090–4095 (1962).
2. R. E. Larsen, W. J. Glover, B. J. Schwartz, Does the hydrated electron occupy a cavity? *Science* **329**, 65–69 (2010).
3. M. H. Elkins, H. L. Williams, A. T. Shreve, D. M. Neumark, Relaxation mechanism of the hydrated electron. *Science* **342**, 1496–1499 (2013).
4. J. V. Coe, G. H. Lee, J. G. Eaton, S. T. Arnold, H. W. Sarkas, K. H. Bowen, C. Ludewigt, H. Haberland, D. R. Worsnop, Photoelectron spectroscopy of hydrated electron cluster anions, $(H_2O)^-_{n=2\text{-}69}$. *J. Chem. Phys.* **92**, 3980–3982 (1990).
5. L. Turi, W.-S. Sheu, P. J. Rossky, Characterization of excess electrons in water-cluster anions by quantum simulations. *Science* **309**, 914–917 (2005).
6. J. R. Verlet, A. E. Bragg, A. Kammrath, O. Cheshnovsky, D. M. Neumark, Observation of large water-cluster anions with surface-bound excess electrons. *Science* **307**, 93–96 (2005).
7. D. Borgis, P. J. Rossky, L. Turi, Electronic excited state lifetimes of anionic water clusters: Dependence on charge solvation motif. *J. Phys. Chem. Lett.* **8**, 2304–2309 (2017).
8. K. R. Siefermann, Y. X. Liu, E. Lugovoy, O. Link, M. Faubel, U. Buck, B. Winter, B. Abel, Binding energies, lifetimes and implications of bulk and interface solvated electrons in water. *Nat. Chem.* **2**, 274–279 (2010).
9. Y. Tang, H. Shen, K. Sekiguchi, N. Kurahashi, T. Mizuno, Y. I. Suzuki, T. Suzuki, Direct measurement of vertical binding energy of a hydrated electron. *Phys. Chem. Chem. Phys.* **12**, 3653–3655 (2010).
10. A. Lübcke, F. Buchner, N. Heine, I. V. Hertel, T. Schultz, Time-resolved photoelectron spectroscopy of solvated electrons in aqueous NaI solution. *Phys. Chem. Chem. Phys.* **12**, 14629–14634 (2010).
11. A. T. Shreve, T. A. Yen, D. M. Neumark, Photoelectron spectroscopy of hydrated electrons. *Chem. Phys. Lett.* **493**, 216–219 (2010).
12. Y. Yamamoto, S. Karashima, S. Adachi, T. Suzuki, Wavelength dependence of UV photoemission from solvated electrons in bulk water, methanol, and ethanol. *J. Phys. Chem. A* **120**, 1153–1159 (2016).
13. D. Luckhaus, Y. I. Yamamoto, T. Suzuki, R. Signorell, Genuine binding energy of the hydrated electron. *Sci. Adv.* **3**, e1603224 (2017).
14. M. Michaud, A. Wen, L. Sanche, Cross sections for low-energy (1-100 eV) electron elastic and inelastic scattering in amorphous ice. *Radiat. Res.* **159**, 3–22 (2003).
15. B. Winter, R. Weber, W. Widdra, M. Dittmar, M. Faubel, I. Hertel, Full valence band photoemission from liquid water using EUV synchrotron radiation. *J. Phys. Chem. A* **108**, 2625–2632 (2004).
16. B. Winter, M. Faubel, Photoemission from liquid aqueous solutions. *Chem. Rev.* **106**, 1176–1211 (2006).

17. K. Nishizawa, N. Kurahashi, K. Sekiguchi, T. Mizuno, Y. Ogi, T. Horio, M. Oura, N. Kosugi, T. Suzuki, High-resolution soft X-ray photoelectron spectroscopy of liquid water. *Phys. Chem. Chem. Phys.* **13**, 413–417 (2011).
18. H. Okuyama, Y. Suzuki, S. Karashima, T. Suzuki, Charge-transfer-to-solvent reactions from I^- to water, methanol, and ethanol studied by time-resolved photoelectron spectroscopy of liquids. *J. Chem. Phys.* **145**, 074502 (2016).
19. J. Kloepfer, V. Vilchiz, V. A. Lenchenkov, A. Germaine, S. E. Bradforth, The ejection distribution of solvated electrons generated by the one-photon photodetachment of aqueous I^- and two-photon ionization of the solvent. *J. Chem. Phys.* **113**, 6288–6307 (2000).
20. F. Messina, O. Bräm, A. Cannizzo, M. Chergui, Real-time observation of the charge transfer to solvent dynamics. *Nat. Commun.* **4**, 2119 (2013).
21. L. Turi, P. J. Rossky, Theoretical studies of spectroscopy and dynamics of hydrated electrons. *Chem. Rev.* **112**, 5641–5674 (2012).
22. K. Yokoyama, C. Silva, D. H. Son, P. K. Walhout, P. F. Barbara, Detailed investigation of the femtosecond pump-probe spectroscopy of the hydrated electron. *J. Phys. Chem. A* **102**, 6957–6966 (1998).
23. M. S. Pshenichnikov, A. Baltuška, D. A. Wiersma, Hydrated-electron population dynamics. *Chem. Phys. Lett.* **389**, 171–175 (2004).
24. A. Thaller, R. Laenen, A. Laubereau, Femtosecond spectroscopy of the hydrated electron: novel features in the infrared. *Chem. Phys. Lett.* **398**, 459–465 (2004).
25. E. P. Farr, C.-C. Zho, J. R. Challa, B. J. Schwartz, Temperature dependence of the hydrated electron's excited-state relaxation. II. Elucidating the relaxation mechanism through ultrafast transient absorption and stimulated emission spectroscopy. *J. Chem. Phys.* **147**, 074504 (2017).
26. C.-C. Zho, B. J. Schwartz, Time-resolved photoelectron spectroscopy of the hydrated electron: Comparing cavity and noncavity models to experiment. *J. Phys. Chem. B* **120**, 12604–12614 (2016).
27. S. Karashima, Y.-i. Yamamoto, T. Suzuki, Resolving nonadiabatic dynamics of hydrated electrons using ultrafast photoemission anisotropy. *Phys. Rev. Lett.* **116**, 137601 (2016).
28. R. Jimenez, G. R. Fleming, P. Kumar, M. Maroncelli, Femtosecond solvation dynamics of water. *Nature* **369**, 471–473 (1994).
29. B. J. Schwartz, P. J. Rossky, The interplay of dielectric and mechanical relaxation in solvation dynamics. *J. Mol. Liq.* **65**, 23–30 (1995).
30. S. Roy, B. Bagchi, Solvation dynamics in liquid water. A novel interplay between librational and diffusive modes. *J. Chem. Phys.* **99**, 9938–9943 (1993).
31. A. A. Mosyak, O. V. Prezhdo, P. J. Rossky, Solvation dynamics of an excess electron in methanol and water. *J. Chem. Phys.* **109**, 6390–6395 (1998).
32. J. Nishitani, C. W. West, T. Suzuki, Angle-resolved photoemission spectroscopy of liquid water at 29.5 eV. *Struct. Dyn.* **4**, 044014 (2017).
33. F. Frassetto, C. Cacho, C. A. Froud, I. E. Turcu, P. Villoresi, W. A. Bryan, E. Springate, L. Poletto, Single-grating monochromator for extreme-ultraviolet ultrashort pulses. *Opt. Express* **19**, 19169–19181 (2011).
34. N. Kurahashi, S. Karashima, Y. Tang, T. Horio, B. Abulimiti, Y.-I. Suzuki, Y. Ogi, M. Oura, T. Suzuki, Photoelectron spectroscopy of aqueous solutions: Streaming potentials of NaX (X= Cl, Br, and I) solutions and electron binding energies of liquid water and X^-. *J. Chem. Phys.* **140**, 174506 (2014).
35. J. V. Coe, A. D. Earhart, M. H. Cohen, G. J. Hoffman, H. W. Sarkas, K. H. Bowen, Using cluster studies to approach the electronic structure of bulk water: Reassessing the vacuum level, conduction band edge, and band gap of water. *J. Chem. Phys.* **107**, 6023–6031 (1997).
36. F. Ambrosio, Z. Guo, A. Pasquarello, Absolute energy levels of liquid water. *J. Phys. Chem. Lett.* **9**, 3212–3216 (2018).
37. A. P. Gaiduk, T. A. Pham, M. Govoni, F. Paesani, G. Galli, Electron affinity of liquid water. *Nat. Commun.* **9**, 247 (2018).
38. V. Ziaei, T. Bredow, Probing ionization potential, electron affinity and self-energy effect on the spectral shape and exciton binding energy of quantum liquid water with self-consistent many-body perturbation theory and the Bethe–Salpeter equation. *J. Phys. Condens. Matter* **30**, 215502 (2018).

Acknowledgments: We thank S. Thürmer for measurements of He(I) photoelectron spectra of methanol and ethanol. **Funding:** This research is supported by JSPS KAKENHI grant no. 15H05753. **Author contributions:** T.S. conceived the study and originated the retrieval method. J.N. and C.W.W. constructed EUV light source and measured the eBE distributions of solvated electrons. Y.-i.Y. performed the data analysis for the retrieval of UV photoelectron spectra. S.K. performed UV photoelectron experiments. **Competing interests:** The authors declare that they have no competing interests. **Data and materials availability:** All data needed to evaluate the conclusions in the paper are present in the paper and/or the Supplementary Materials. Additional data related to this paper may be requested from the authors.

Submitted 16 January 2019
Accepted 24 July 2019
Published 30 August 2019
10.1126/sciadv.aaw6896

Citation: J. Nishitani, Y.-i. Yamamoto, C. W. West, S. Karashima, T. Suzuki, Binding energy of solvated electrons and retrieval of true UV photoelectron spectra of liquids. *Sci. Adv.* **5**, eaaw6896 (2019).

Binding energy of solvated electrons and retrieval of true UV photoelectron spectra of liquids

Junichi Nishitani, Yo-ichi Yamamoto, Christopher W. West, Shutaro Karashima and Toshinori Suzuki

Sci Adv **5** (8), eaaw6896.
DOI: 10.1126/sciadv.aaw6896